OBJECT ORIENTED EXTRACTION OF WETLANDS BASED ON SYNERGISTIC USE OF MULTISPECTRAL AND MICROWAVE REMOTE SENSING DATA

R. Leiterer[(1)], J. Kropacek[(2)], F. Chen[(4)], C. Thiel[(3)], P. Krause[(1)], V. Hochschild[(2)], J. Helmschrot[(1,5)]

[(1)]Friedrich-Schiller-University Jena, Institute of Geography, Department of Geoinformatics, Hydrology and Modelling, Grietgasse 6, 07745 Jena, Germany, Email: reik.leiterer@uni-jena.de
[(2)]Tuebingen University, Institute of Geography, Department of Geoinformatics, Ruemelinstr. 19-23, 72070 Tuebingen, Germany, Email: jan.kropacek@uni-tuebingen.de
[(3)]Friedrich-Schiller-University Jena, Institute of Geography, Department of Earth Observation, Grietgasse 6, 07745 Jena, Germany, Email: christian.thiel@uni-jena.de
[(4)]Chinese Academy of Science, Institute of Tibetan Plateau Research, Key Laboratory of Tibetan Environment Changes and Land Surface Processes, Beijing 100085, China, Email: fech@itpcas.ac.cn
[(5)]University of Washington, Department of Civil and Environmental Engineering, Mountain Hydrology Research Group, 111 Wilson Ceramics Lab,Box 352700, Seattle, WA, 98195, USA, Email: jhelmsch@uw.edu

ABSTRACT

The Tibetan Plateau (TP) is identified as a global climate change hotspot due to its relevance for the Asian monsoon circulation system. Glacial melt and receding permafrost indicate significant changes within this climate system. Spatio-temporal information is required to gain a better understanding of the interactions of system components and ongoing processes. By numerous studies, Earth Observation data analysis has been shown as being a suitable tool which enables to monitor mid- and long-term environmental changes. A new object oriented classification approach which is based on synergies between the optical remote sensing products and SAR data was developed for automatic and seasonal-adaptive extraction of parameters for wetland area derivation and characterization. It was shown that the derived parameters are important indicators for environmental change analyses. The developed method is appropriate to monitor wetland responses with high temporal and spatial resolution according to climate change and human impacts within large regions like the TP.

1. INTRODUCTION

Many studies suggest that the TP is one of the most sensitive areas in responding to global climate change but only little knowledge is given on the impact of likely changing monsoon dynamics on past, recent and future process dynamics within the eco-hydrological system [1, 2, 3]. Due to the general characterization of wetlands as a dynamic ecosystem that is vulnerable to climate-driven changes in hydrological systems, this study focuses on wetland monitoring within the Lake Nam Co catchments. Those wetlands are assumed to play an important role in the catchment water balance by affecting runoff and evapotranspiration dynamics. The loss of wetlands in this region would have serious consequences for the local community, thus. Since Earth Observation (EO) based data allow to identify environmental and in particular eco-hydrological drivers, they can also be used to develop indicators for environmental impact assessment approaches [4].
The research approach used in this study combines field observations, hydrological parameter derivation based on multi-sensoral and multi-temporal remote sensing data (TerraSAR-X, Envisat ASAR/ MERIS, ERS-1/2 Tandem Pairs, ALOS PalSAR, Landsat TM/ETM+) as well as terrain analyses from Digital Elevation Models. Since parameters like temperature, phenology and soil moisture are recognized as suitable indicators for environmental change analyses, their spatio-temporal estimates has been used to monitor changes in wetland and permafrost in this semi-arid region.

1.1. Project Background

The presented study is part of the DFG Priority Programme 1372 “Tibetan Plateau: Formation-Climate-Ecosystems” (TiP) and focuses on a better understanding of the driving forces controlling eco-hydrological processes in the context of a likely changing climate and monsoon dynamic in Asian high-altitude environments. Due to its impacts on the Asian Monsoon System, the Tibetan Plateau plays a key role for global climate dynamics and, thus, is characterized as a climate change hotspot by the Intergovernmental Panel on Climate Change (IPCC) [5]. Therefore, one objective of this interdisciplinary project is to identify eco-hydrological feedbacks to changing climate conditions by analyzing and modelling its underlying spatially and temporally variable hydrological components and processes on the TP.

Proc. ‘ESA Living Planet Symposium’, Bergen, Norway
28 June – 2 July 2010 (ESA SP-686, December 2010)

1.2. Study Area: Nam Co Basin

Being representative for close hydrologic systems of central Tibet, the Nam Co Basin is an endorheic drainage system that belongs to the zone of seasonal, sporadic/island permafrost [6]. The Lake Nam Co is located at 4718 m a.s.l. (30°N, 90°E). In 2005, the Nam Co Station for Multisphere Observation and Research (NAMOR) was established for environmental long-term monitoring in the central TP (Fig. 1).

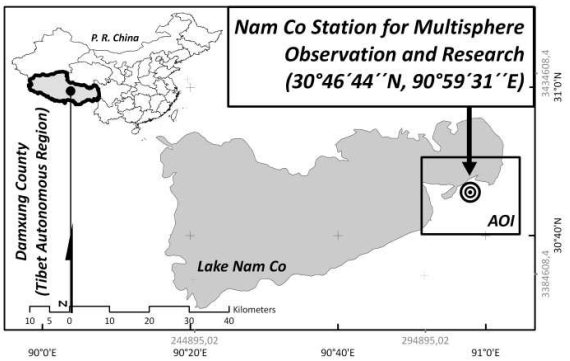

Figure 1. Area of Interest (AOI) in the Lake Nam Co drainage system

The climate in the Nam Co catchment is characterized by a mean average temperature of 0°C with large seasonal and daily variations (Fig. 2) [7]. In the summer season (Jun – Sep), the study area is characterized by the influence of the Indian summer monsoon. This leads to high precipitation rates (about 70% of annual precipitation) and relatively higher temperature with the maximum monthly mean temperature in July [8]. Thus, the growth period is confined to this season. In autumn (Oct-Nov) there is a decrease of precipitation. The winter (Dec-Feb) and spring (Mar-May) seasons are very cold and they are characterized by comparable low precipitation [9].

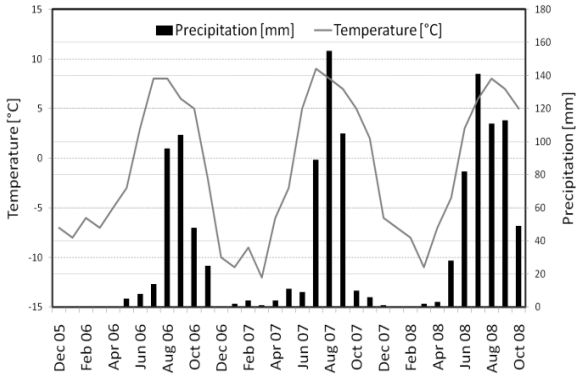

Figure 2. Mean monthly temperature and precipitation recorded at NAMOR (December 2005 - October 2008)

The main vegetation in the study area includes *Kobresia pygmaea* and *Stipa* dominated alpine meadows and *Kobresia schoenoides* wetlands with a hummock-like structure. Those areas are considerably affected by likely irreversible degradation mainly caused by rising temperatures and extensive overgrazing [10].

1.3. Available Data

A set of SAR data including ENVISAT ASAR data acquired in AP mode (HH/HV), ERS-1/2 tandem pairs, ALOS PALSAR FBD images and TerraSAR-X data in StripMap mode (VV/VH) were used in this study. Also, optical data such as Landsat scenes, MERIS FR and MODIS data were processed. For data processing, classification and parameterization purposes, the digital elevation models of the Shuttle Radar Topography Mission (SRTM) and the ASTER Global Digital Elevation Map (GDEM) were combined (Tab. 1).

Table 1. Summary of used EO datasets

SAR Data		***Date***
	ERS-1/2 Tandem	Apr 1996
	ENVISAT ASAR	Apr 2005
	ALOS PALSAR	Aug 2009
	TerraSAR-X	Aug 2009
Optical Data		
	Landsat	Sep 1991 – Aug 2007
	MERIS	Dec 2004 - Jun 2006
DEM		
	SRTM V4	2000
	ASTER GDEM	since 2000

A variety of coarser scale land cover products as well as the National Land Cover Database 2000 (NLCD) of China were available for the whole catchment and were explored as reference data. In addition, hydrological, biophysical and texture measurements were carried out at more than 130 sample plots in the eastern part of the Nam Co area during several field campaigns in 2009.

2. PRE-PROCESSING OF DATA

Initially, the EO-data was pre-processed on the basis of common techniques using the software packages *GAMMA Remote Sensing* and *PCI Geomatica*. The SAR data were radiometric calibrated (including speckle filtering), geocoded and reprojected. Due to the sensitivity of the backscattering coefficient to the terrain a topographic normalization was performed [11]. To reduce the speckle effect for an adequate estimate of σ^0, the Frost filter was applied. The performance of speckle reduction has been evaluated on the basis of filter and speckle noise indices and the Equivalent Number of Looks (ENL). Additionally, the Edge Keeping Index was used to verify texture and edge preservation [12]. Because of the limited availability of SAR scenes, a

suitable application of multi-temporal filtering was impossible.

To retrieve physical parameters from Landsat data, e.g. surface reflectance and surface temperature, the elimination of atmospheric and illumination effects is essential and was realized by the atmospheric/topographic correction utilizing ATCOR3 algorithm [13], providing the corresponding surface reflectance channels, surface emissivity and brightness temperature for the thermal bands as well as biophysical vegetation parameters such as the Soil Adjusted Vegetation Index (SAVI) and the Leaf Area Index (LAI) (a_0, a_1, a_2 = vegetation specific parameter set) (Eq. 1-2) [14]. Based on those vegetation indices, vegetation dynamics and phenology were characterized and vegetation and non-vegetation areas were mapped.

$$SAVI = \frac{(Landsat_{Band\,4} - Landsat_{Band\,3}) * 1.5}{(Landsat_{Band\,4} + Landsat_{Band\,3} + 0.5)} \quad (1)$$

$$LAI = -\frac{1}{a_2} \ln \frac{(a_0 - SAVI)}{a_1} \quad (2)$$

GlobCover MERIS FR composites were used, to provide the mean surface reflectance from all valid observations for each band within the respective 2 months period. This GlobCover product includes geometric correction of the input data, cloud screening, shadow detection and atmospheric as well as BRDF (Bidirectional Reflectance Distribution Function) correction [15]. For MERIS, the NDVI and the SAVI were calculated from the bands 13 (865 nm) and 7 (665 nm). Due to its sensitivity to varying chlorophyll contents, the MERIS Terrestrial Chlorophyll Index (MTCI) was calculated (Eq. 3) allowing a good distinction between different photosynthetic activities [16].

$$MTCI = \frac{(MERIS_{Band\,10} - MERIS_{Band\,9})}{(MERIS_{Band\,9} + MERIS_{Band\,8})} \quad (3)$$

In relation to the first-order control of topography to the spatial variations of hydrological conditions, the topographic parameters slope, aspect and Topographic Wetness Index (TWI) were calculated [17]. Slope parameters provide information on runoff generation mechanisms, while the aspect indicates spatial variations in evapotranspiration. Since the TWI is calculated by the specific catchment area α (the cumulative upslope area draining through a certain point per unit contour length) and the local slope $tan\,\beta$ (Eq. 4), it is a relative measure often used for the delineation of soil moisture pattern [18].

$$TWI = ln\left(\frac{\alpha}{tan\beta}\right) \quad (4)$$

3. METHOD

To extract and distinguish different wetland types, three classification approaches were explored. Supervised (Maximum Likelihood Classification), unsupervised (k-means clustering) and rule based (object oriented) classifications were performed by the combined analysis of optical bands, the SAR intensity information as well as vegetation indices and topographic parameters. The comparison and analysis of the classification results pointed out that the multi-resolution, object oriented analysis approach using *eCognition* will provide most reliable results for the wetland classification and characterization. In *eCognition* the multi-resolution segmentation is a stepwise bottom-up region merging process accounting for the weighted heterogeneity and the defined object size. The resulting simultaneous growth of segments leads to adjacent image objects of comparable scale [19]. The concept for the field-based wetland distinction (Ch. 3.1) and the wetland classification approach (Ch. 3.2) are presented below.

3.1. Field-based Wetland Distinction

To distinguish wetlands by remote sensing data analysis, knowledge about the expected wetland types is necessary. During several field campaigns in 2009, measurements and drillings at 68 plots have been carried out in the wetland areas. It was shown that wetlands occur in altitudes between 4700 and 5100 m asl. and are characterized by a hummocky micro-topography. They can be formed in either flat areas, but also on steep slopes with gradients higher than 10°. A combined process of peat formation and root penetration/accumulation results in deep top soil horizons which are rich in rhizogenic, organic matter [20].

The wetlands located near the lakeshore and river estuaries (hereafter referred to as *type I*) are affected by fluctuating groundwater, but also annual lake level changes (> 70 cm/ year) and the current process of continuous lake level rise [21]. However, this wetland type is characterized by permanent water saturation and a high amount of open water bodies. A second wetland type (*type II*) was identified along the footslope areas of the surrounding mountains. This type is characterized by a well-developed hummock structure. Due to its heterogeneity some parts become dry during the summer season whereas other parts are permanently saturated. In the dry parts, no frozen layer was detected by sounding in August and October. However, drilling indicate that subsurface water is confined by an overlying, relatively impermeable layer [22]. Small isolated wetland patches formed in sinks and gully-like river valleys at higher altitudes (above 4850 m a.s.l) were defined as wetland *type III*. Those wetlands can also be connected to *type II*. Due to the steep gradient,

the influence of groundwater decrease and the stagnant soil water regime is driven by a permanent frozen layer. Based on drilling results in August, the active layer thickness in a selected part of a wetland *type III* (30°43′05″N, 90°03′36″E / 4950 - 5050 a.s.l) varies by a depth of 40 to 90 cm, whereas in the conterminous regions no frozen layer up to 110 cm exists. This suggests that the extent of *type III* correlates with the extent of the permanent frozen layer. Based on findings, for example regarding the likely impact of frozen layers on wetland formation, a wetland differentiation by earth observation data should include thermal information, phenology dynamics and texture analysis.

3.2. Wetland Classification Approach

The basic principle of the classification approach is the processing of multi-scale image object layers. The initial segmentation level was generated using a *scale* parameter of „10", a *shape* parameter of „0.1" and a high *compactness* of „0.7". As input layers, the visible, near infrared and panchromatic bands as well as the calculated vegetation indices were included. In this level the classification of the parent classes *water*, *vegetation* and *other* is intended. Below the parent class *vegetation,* a second segmentation level was generated by using a *scale* parameter of „5", a high influence of color on the segmentation process (*shape* „0.1") and less compact image objects (*compactness* „0.3"). Focusing on a robust wetland classification, thermal information, vegetation indices and the vegetation sensitive Landsat bands 2, 3 and 4 were included as input layers. To subdivide the *wetland* class, three new child classes were inserted into the hierarchical classification tree (*type I*, *type II* and *type III)*. Based on the generated image objects, the hierarchical classification concept was realized (Fig. 3). In order to achieve a high transparency and transferability, the derived parent classes were coded according to the land cover classification system (LCCS) [23].

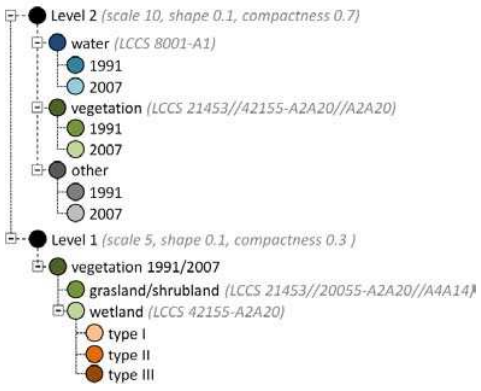

Figure 3. Simplified hierarchical classification concept developed in eCognition including standard LCCS description for the parent classes (Code-LCC formula)

The *eCognition* feature space optimization tool, a method to mathematically calculate the best combination of features in the feature space, was explored to receive the most relevant features for the classification. Thus, the parent classes *vegetation*, *water* and *other* were separated for 1991 and 2007 at the coarse scale level (Level 2). Within a maximal 5-dimensional separating feature space and using ~ 500 object features such as the normalized layer values, vegetation indices, ratios and texture, the feature optimization was applied. A best overall separation distance higher than ´5.0´ for 1991 and 2007 shows the largest distance between the closest samples of the respective classes. Thus, the resulting optimized features for the class description in Fig. 4 include SAVI, NDVI, the mean layer value of the Landsat bands 1 (blue) and 3 (red) as well as the all directional entropy of the grey level co-occurrence matrix (GLCM) [24].

Class/Class	vegetation	other	water
vegetation	0.00	5,28	5,20
other	5,28	0.00	6,56
water	5,20	6,56	0.00

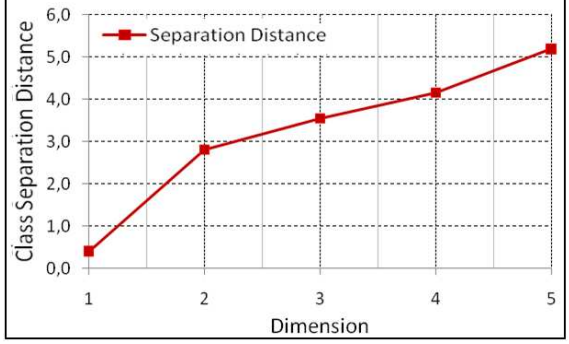

Figure 4. Class separation distance matrix and separation chart for Level 2 classification (1991)

The parent class *vegetation* was subdivided by using the same way at the finer scale (Level 1) into the classes *grassland/shrubland* and *wetland*. Due to the thematic similarity of the target classes, a more complex 10-dimensional separating feature space was used, resulting in a best separation distance of ´5.3´ (Fig. 5).

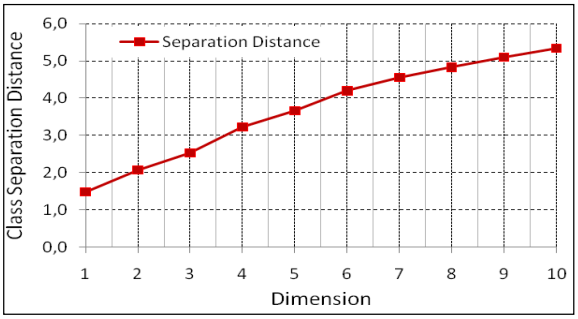

Figure 5. Separation chart for Level 1 classification

The optimized features for the class distinction include vegetation indices as well as texture information of the middle and thermal infrared bands and the SAR data intensities (Tab. 2).

Table 2. Features used for class differentiation of grassland/shrubland and wetland

Thermal Infrared (mean layer value)	***Vegetation Indices***	***Texture (according to Haralick)***
Landsat band 61 (Dec - 2000)	Landsat NDVI (Sep - 1991/ Aug - 2007)	Homogeneity (Landsat band: 5, 61, 7 – Dec 2000)
Landsat band 62 (Dec - 2000)	Landsat SAVI (Sep - 1991/ Aug - 2007)	Entropy all dir. (Landsat band: 5 – Dec 2000)
		SAR intensity (X-Band, C-Band, L-Band)

With this feature space, a nearest neighbor classifier for the chosen classes was created and the images were classified for each Landsat acquisition time step in the vegetation period. From this effort, a map showing the spatial distribution of *wetland* and *grassland/shrubland* areas was generated (Fig. 6).

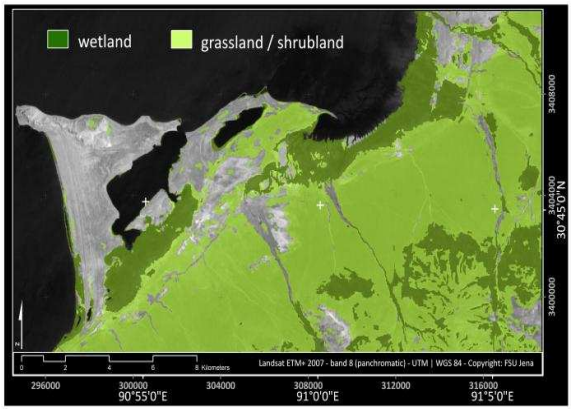

Figure 6. Classification of wetland and grassland/shrubland areas for 2007

A cross-comparison of the classification results pointed out the frequency of wetland changes between 1991 and 2007. On this topic, reference is made to [22].

For further differentiation of the derived basic *wetland* class, a complex rule-set was developed, including all vegetation indices, SAR texture information and phenology characteristics. On the basis of the field-based wetland classification, those different features were evaluated with regard to their suitability of wetland type extraction (Tab. 3).

Table 3. Features to be considered for wetland type specification and differentiation

Feature	***Adapted for separation of***
MERIS vegetation indices	*type I, II* from *type III*
Landsat thermal features	*all types*
Landsat vegetation indices	*type I, II* from *type III*
SAR texture/intensity features	*type II* from *type I, III*
DEM features	*all types*

4. RESULTS AND VALIDATION

The MERIS bimonthly NDVI, SAVI and MTCI products (Nov 2004 – Jun 2006) are strongly related to specific vegetation dynamics, depending on the yearly rain and temperature cycle. It was found, that compared to *type I, II* the vegetation indices for *type III* follows the general growth period with a temporal delay and a maximum severability in the time period May to June. Thus, the vegetation dynamics are useful for the separation of *type III* from other wetland areas. However, due to the coarse spatial resolution of 300 m, a complete detection of these small wetland patches did not provide sufficient results. The Landsat vegetation indices SAVI, NDVI and LAI might be useful to delineate those small patches, but the sensitive period for the separation of vegetation characteristics was not covered by the available data set yet. From this effort, it can be concluded that the accurate delineation of the identified wetland types based on vegetation dynamics require high temporal and spatial resoluted data. The use of data from satellite missions such as RapidEye, Sentinel-2 or FORMOSAT offers a great potential for such vegetation related approaches and needs to be further explored.

The Landsat thermal features were analyzed by considering mean layer values, standard deviation and homogeneity. While a difference in temperature between grassland and wetlands could be determined, the variations in temperature within wetland classes show only a non-significant correlation between the wetland types *II*, *III* and type *I*. It is assumed that further analyses using data with better temporal and spatial resolution will improve the classification results.

The analysis of features based on the SAR data showed that the *grassland/shrubland* and the basic *wetland* class can be distinguished. It is further indicated that neither the texture information nor the intensities of the C- and X-band data allow a reliable identification of the target wetland type classes. However, since the ALOS L-band information content showed slight sensitivity to different wetland types (Fig. 7), a separation between *type I, II*, and *type III* was carried out by using a combination of intensity and texture information (all directional homogeneity and entropy) of the HH/HV–ratio.

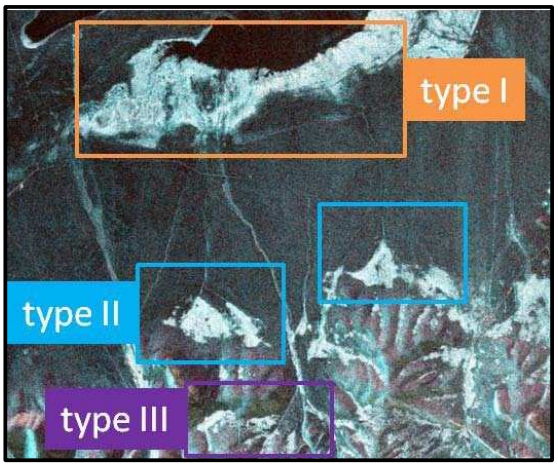

Figure 7. ALOS PALSAR FBD false color composite of HH/HV and HH intensities – the figure shows the more homogeneous structure and the higher intensities in areas of wetland type II and III in comparison to type I

Enhancing the information on wetlands distributed in the study area, parameters derived from relief analysis were integrated. Here, the mean height and slope parameters were identified as being useful to distinguish the three wetland types (Fig. 8). Due to the specific geomorphologic characteristics of *type III* wetlands (see Ch. 3.1); the TWI was assumed to enable a better discretization between *type II* and *type III*.

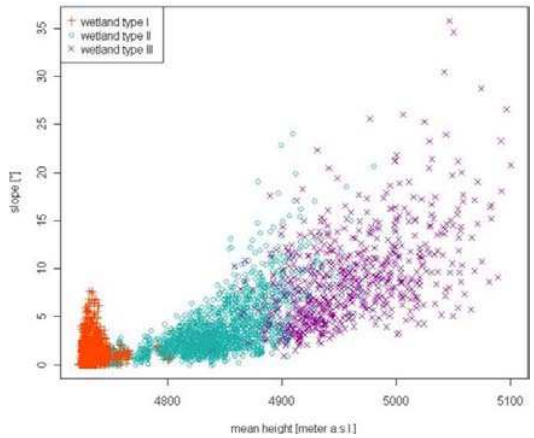

Figure 8. Feature space of mean slope and height for the different wetland types in the area of interest

The resulting classification approach has been carried out on the basis of a nearest neighbor classifier on a fuzzy logic basis. Since in reality the wetland types merge seemingly seamlessly, this fuzzy concept is considered to be the best in solving the difficult task of wetland type separation. Thus, each wetland type object shows the degree of assignment to all wetland classes. The classification result shows the spatial distribution of the three target wetland type classes with specific class assignments of > 50 % (Fig. 9).

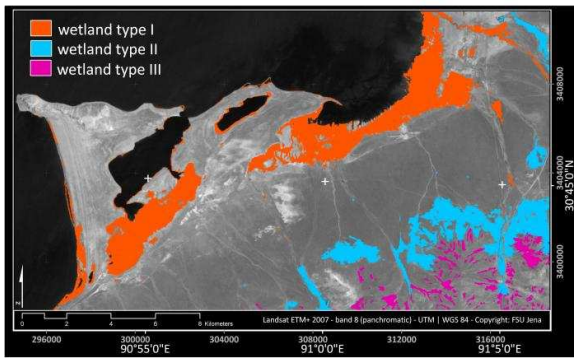

Figure 9. Resulting wetland type classification

The wetland map was validated integrating extensive in-situ measurements and a multi-scale comparative assessment approach utilizing complementary Earth Observation products (e.g. GlobCover, NLCD). In consequence of the lack of required thematically depth of the Earth Observation products, the comparison was conducted on the basis of the parent wetland class only. The wetland map features a very poor agreement with the land cover products, although, this result originates from the moderate thematic and spatial accuracy of the coarser scale land cover products. In comparison to the in-situ measurements in the area of interest, an overall accuracy of 92 % could be achieved for the parent wetland class and 84 % for the three different wetland types, even though uncertainties remain due to the limited ground information especially for the wetland *type III*.

However, those results indicate that the developed classification approach provides reliable results for wetland mapping and long-term monitoring on the Tibetan Plateau, but also that available land cover products lack in accuracy in such highly dynamic environmental systems.

5. CONCLUSIONS

The results show, that a combination of remote sensing data from multiple sensors and topographic information enables accurate mapping of wetlands and wetland types. Using an object oriented classification approach multiplicities of features were evaluated in terms of their suitability for wetland characterization, but often turned out to be unsatisfactory for the desired classification depth of different wetland types. For example, the vegetation dynamics and thermal characteristics seem to have great potential, once accordant datasets with high temporal and spatial resolution are available. In general, SAR data features are very useful for the identification of the basic wetland class. For further differentiation of wetland types, only the L-band data lead to the desired results. However, the DEM features, i.e. *height*, *slope* and *TWI* were analyzed to better distinguish between the three

wetland types. In combination with SAR features, this approach allows an accurate mapping of different wetland types as shown by the validation of the wetland map with field data.

This study has also shown that, the relationship between surface properties and the specific underlying impermeable layers (e.g. permafrost or layer of clay) as well as the interaction between surface and subsurface process dynamics need to be better understood and integrated by further studies. EO data with high spatial and temporal resolutions are assumed to be useful to better identify wetland areas affected or driven by underlying permafrost, but also to monitor and assess changes related to increasing temperatures or human activities.

6. ACKNOWLEDGMENTS

This research work is part of the DFG priority program 1372 Tibetan Plateau: Formation - Climate - Ecosystems (TiP). Acknowledgement is given to the Institute of Tibetan Plateau Research for data and logistical support in the field. The ENVISAT MERIS data has been obtained from the ESA/ESA GlobCover Project, led by MEDIAS-France.

7. REFERENCES

1. An, Z., Kutzbach, J.E., Prell, W.L. & S.C. Porter (2001). Evolution of Asian monsoons and phased uplift of the Himalaya-Tibetan plateau since Late Miocene times, *Nature*, **411,** pp 62–66.

2. Du, M., Kawashima, S., Yonemura, S. , Zhang, X. & S. Chen (2004). Mutual influence between human activities and climate change in the Tibetan Plateau during recent years, *Global and Planetary Change*, **41**(3-4), pp 241-249.

3. Liu, X.D. & B.D. Chen (2000). Climatic warming in the Tibetan Plateau during recent decades, *International Journal of Climatology*, **20,** pp 1729–1742.

4. Xue, X., Guo,, J., Han, B., Sun, Q. & L. Liu (2009). The effect of climate warming and permafrost thaw on desertification in the Qinghai-Tibetan Plateau, *Geomorphology*, **108**(3-4), pp 182-190.

5. IPCC (2007). *Climate Change 2007: The Physical Science Basis*, Cambridge University Press, Cambridge, UK.

6. Keil, A., Berking, J., Mugler, I., Schutt, B., Schwalb, A. & P. Steeb (2010). Hydrological and geomorphological basin and catchment characteristics of Lake Nam Co, South-Central Tibet, *Quaternary International*, **218**(1-2), pp 118-130.

7. Zhang, Y., Kang, S. & M. Li (2008). Climatic features at Nam Co station, Tibetan Plateau. *Annual Report of Nam Co Station for Multisphere Observation and Research, CAS,* **3**, pp 1-8.

8. Cong, Z., Kang, S., Smirnov, A. & B. Holben (2009). Aerosol optical properties at Nam Co, a remote site in central Tibetan Plateau, *Atmospheric Research*, **92**(1), pp 42-48.

9. You, Q., Kang, S., Li, C., Li, M. & J. Liu (2007). Variation features of meteorological elements at Namco Station, Tibetan Plateau, *Meteorological Monthly*, **33**, pp 54–60.

10. Arthur, A.D., Pech, R.P., Zhang, Y. & Lin, H. (2007). Grassland degradation on the Tibetan Plateau: the role of small mammals and methods of control. ACIAR *Technical Reports*, **67**, pp 1-35.

11. Castel, T., Beaudoin, A., Stach, N. & N. Stussi (2001). Sensitivity of Space-Borne SAR Data to Forest Parameters over Sloping Terrain. Theory and experiment, *Int. J. Remote Sens*., **22**, pp 2351-2376.

12. Zhiyong, W., Jixian, Z. & W. Tongxiao (2004). The contrast research of the methods of restraining the speckle noise of SAR images, *XXth ISPRS Congress, 12-23. July, Istanbul, Turkey.*

13. Song, C., Woodcock, C.E., Seto, K.C., Lenney, M.P. & S.A. Macomber (2001). Classification and Change Detection Using Landsat TM Data: When and How to Correct Atmospheric Effects?, *Remote Sens. Environ*., **75**, pp 230-244.

14. Richter, R. (2008). Atmospheric/ Topographic Correction for Satellite Imagery, *DLR report,* DLR-IB 565-01/08, Wessling, Germany.

15. Bicheron, P., Defourny, P., Brockmann, C., Schouten, L., Vancutsem, C., Huc, M., Bontemps, S., Leroy, M., Achard, F., Herold, M., Ranera, F. & O. Arino (2008). GlobCover: products description and validation report, *ESA GlobCover project*, ftp://uranus.esrin.esa.int/pub/GlobCover _v2/.

16. Dash, J. & P.J. Curran (2007). Evaluation of the MERIS terrestrial chlorophyll index (MTCI), *Advances in Space Research*, **39**(1), pp 100-104.

17. Grabs, T., Seibert, J., Bishop, K. & H. Laudon (2009). Modeling spatial patterns of saturated areas: A comparison of the topographic wetness index and

a dynamic distributed model, *Journal of Hydrology*, **373**(1-2), pp 15-23.

18. Beven, K.J. & M.J. Kirkby (1979). A physically based, variable contributing area model of basin hydrology, *Hydrologic Science Bulletin*, **24**, pp 43–69.

19. Benz, U.C., Hofmann, P., Willhauck, G., Lingenfelder, I. & M. Heynen (2004). Multi-resolution, object-oriented fuzzy analysis of remote sensing data for GIS-ready information, *ISPRS Journal of Photogrammetry and Remote Sensing*, **58**(3-4), pp 239-258.

20. Kaiser, K., Miehe, G., Barthelmes, A., Ehrmann, O., Scharf, A., Schult, M., Schlutz, F., Adamczyk, S. & B. Frenzel (2008). Turf-bearing topsoils on the central Tibetan Plateau, *China: Pedology, botany, geochronology, CATENA*, **73**(3), pp 300-311.

21. Zhou, S., Kang, S., Liu, J. & S. Wang (2006). Preliminary results for hydrological observations in the Nam Co drainage area. *Annual Report of Nam Co Station for Multisphere Observation and Research, CAS,* **1**, pp 55-57.

22. Kropáček, J., Ye, Q., Leiterer, R. & V. Hochschild (2009). Multi-resolution synergy of optical, thermal and SAR data for mapping of wetlands and permafrost on Tibetan Plateau, *Proceedings of Earth Observation and Water Cycle Science Symposium*, 18 – 20 November 2009, Frascati, Italy.

23. Di Gregorio, A. & L. J. M. Jansen (2000). Land cover classification system (LCCS): *Classification concepts and user manual*, Environment and Natural Resources Service, GCP/RAF/287/ITA Africover-East Africa Project and Soil Resources, Management and Conservation Service, Food and Agriculture Organization.

24. Haralick, R.M., Shanmugam, K. & I. Dinstein (1973). Textural Features for Image Classification, *IEEE Transactions on Systems, Man and Cybernetics*, **3**(6), pp 610-620.